# Role of Aspartate 143 in *Escherichia coli* tRNA-Guanine Transglycosylase: Alteration of Heterocyclic Substrate Specificity†

Katherine Abold Todorov‡ and George A. Garcia*

*Department of Medicinal Chemistry, College of Pharmacy, University of Michigan, Ann Arbor, Michigan 48109-1065*

*Received September 13, 2005; Revised Manuscript Received November 3, 2005*

ABSTRACT: tRNA-guanine transglycosylase (TGT) is a key enzyme involved in the post-transcriptional modification of certain tRNAs in their anticodon wobble positions with queuine. To maintain the correct Watson−Crick base pairing properties of the wobble base (and hence proper translation of the genetic code), TGT must recognize its heterocyclic substrate with high specificity. The X-ray crystal structure of a eubacterial TGT bound to preQ$_1$ [Romier, C., et al. (1996) *EMBO J. 15*, 2850−2857] suggested that aspartate 143 (*Escherichia coli* TGT numbering) was involved in heterocyclic substrate recognition. Subsequent mutagenic and computational modeling studies from our lab [Todorov, K. A., et al. (2005) *Biophys. J. 89* (3), 1965−1977] provided experimental evidence supporting this hypothesis. Herein, we report further studies probing the differential heterocyclic substrate recognition properties of the aspartate 143 mutant TGTs. Our results are consistent with one of the mutants exhibiting an inversion of substrate recognition preference (xanthine vs guanine) relative to that of the wild type, as evidenced by $K_m$ values. This confirms the key role of aspartate 143 in maintaining the anticodon identities of the queuine-containing tRNAs and suggests that TGT mutants could be developed that would alter the tRNA wobble base base pairing properties.

There are approximately 100 modified nucleosides that occur in RNA, with the vast majority of them occurring in tRNAs (*1*). The tRNA anticodon is one "hot spot" for hypermodification (e.g., the incorporation of elaborately modified nucleosides). Queuine (Figure 1) is one example of a hypermodified base that occurs in the wobble position of the anticodon of tRNA Asp, Asn, His, and Tyr. Queuine is incorporated into tRNA via a base exchange reaction (replacing guanine) catalyzed by tRNA-guanine transglycosylase (TGT).[1] In eukaryotes, queuine is directly exchanged into tRNA, while in eubacteria, a queuine precursor (preQ$_1$, Figure 1) is incorporated and ultimately modified to queuine (*2*). Queuine, guanine, and preQ$_1$ all share the same 2-aminopyrimidin-4-one moiety that is involved in the Watson−Crick-type base pairing between the tRNA anticodon and the mRNA codon during translation. To accurately maintain this interaction, and hence the identity of the tRNAs and the fidelity of translation, TGT must exercise precise and specific recognition of its heterocyclic substrate.

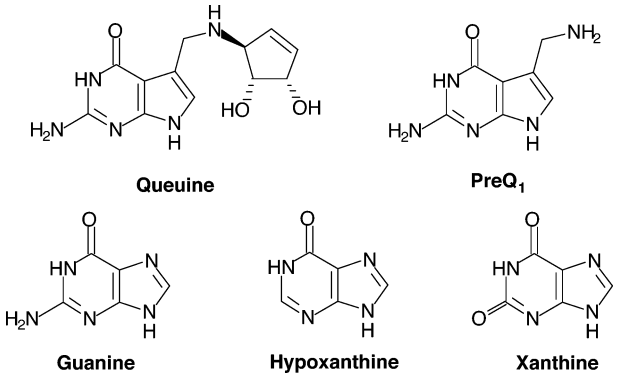


FIGURE 1: Physiological and potential alternative heterocyclic substrates for TGT.

The X-ray crystal structure of the *Zymomonas mobilis* TGT bound to preQ$_1$ revealed that aspartate 143 (D143, *Escherichia coli* TGT numbering) appears to make two hydrogen bonds to the aminopyrimidone portion of preQ$_1$ (*3*). To experimentally probe the role of D143 in heterocyclic substrate recognition, we carried out a thorough biochemical and computational characterization of wild-type and D143 mutant TGTs. Their interactions with guanine confirmed that D143 does play a vital role in heterocyclic substrate recognition (*4*). Computational simulations of guanine binding to wild-type and D143 mutant TGTs provided insight into which interactions assisted in binding guanine (*4*). Since D143 was ascertained to be the determinant for guanine specificity, it follows that mutating this residue may allow

† This work was supported in part by the National Institutes of Health (Grant GM065489 to G.A.G.) and the University of Michigan, College of Pharmacy, Vahlteich Research Fund (G.A.G.). K.A.T. acknowledges the support of the Chemistry-Biology Interface Training Program (GM08597).

* To whom correspondence should be addressed: Department of Medicinal Chemistry, College of Pharmacy, University of Michigan, Ann Arbor, MI 48109-1065. Telephone: (734) 764-2202. Fax: (734) 763-5633. E-mail: gagarcia@umich.edu.

‡ Present address: Armed Forces Institute of Pathology, Rockville, MD 20850.

[1] Abbreviations: TGT, tRNA-guanine transglycosylase; PCR, polymerase chain reaction; DTT, dithiothreitol; HEPES, hydroxyethylpiperazine ethylsulfonate; Tris-HCl, tris(hydroxymethyl)aminomethane hydrochloride; SDS, sodium dodecyl sulfate; PAGE, polyacrylamide gel electrophoresis; TCA, trichloroacetic acid; ECY, *Escherichia coli* tRNA$^{tyr}$ transcript; htTGT(wt), histidine-tagged wild-type TGT. Histidine-tagged TGT mutant enzymes are named according to the pattern htTGT(D143A) (i.e., aspartate 143 mutated to alanine).

10.1021/bi051863d CCC: $33.50 © 2006 American Chemical Society
Published on Web 12/15/2005

Table 1: Solubility Determination of Hypoxanthine and Xanthine[a]

| compound | wavelength (nm) | absorption coefficient ($\epsilon$) ($cm^{-1}\ \mu M^{-1}$) | limit of solubility (mM) |
|---|---|---|---|
| hypoxanthine | 250 | $10.55\ (0.02) \times 10^{-3}$ | ~2 |
| xanthine | 225 | $4.71\ (0.04) \times 10^{-3}$ | ~1.5 |

[a] Solubilities were determined spectrophotometrically in assay buffer [100 mM HEPES (pH 7.3), 20 mM $MgCl_2$, and 5 mM DTT] as described in Materials and Methods. Standard errors are given in parentheses.

for alternate substrate recognition. Not only is there precedence for altering substrate specificity with guanine binding proteins using hypoxanthine and xanthine (Figure 1) (*5*−*7*), but these purines are readily available in vivo and therefore provide an interesting and physiologically relevant study of substrate specificity. We herein report biochemical studies to probe the recognition between wild-type and D143 mutant TGTs and the alternate purine heterocycles, hypoxanthine and xanthine.

## MATERIALS AND METHODS

*Reagents.* Reagents were purchased from Sigma-Aldrich unless otherwise noted. Dithiothreitol (DTT) was obtained form Gibco BRL. HEPES (1 M solution, pH 7.3) was from Amersham Pharmacia. [8-$^3$H]Guanine (1−10 Ci/mmol), [8-$^3$H]xanthine (9 Ci/mmol), and [2,8-$^3$H]hypoxanthine (24.2 Ci/mmol) were purchased from Moravek Biochemicals, Inc. Whatman GF/C 24 mm glass microfiber filters were obtained from Fisher Scientific. Biodegradable liquid scintillation counting cocktail Bio-Safe II was from Research Products. Wild-type and mutant TGTs were expressed and purified with amino-terminal histidine tags as described previously (*4*). On the basis of SDS−PAGE analysis (not shown), the mutants were free of any detectable, contaminating wild type. *E. coli* $tRNA^{Tyr}$ (ECY) was prepared via in vitro transcription as previously described (*8*) and purified under native conditions by anion exchange chromatography.

*Determination of the Concentrations and Solubilities of Hypoxanthine and Xanthine.* Because of the high hypoxanthine and xanthine concentrations that are necessary for the TGT kinetics, the solubility of these compounds was tested at pH 7.3. Excess hypoxanthine or xanthine was added to a mixture containing 100 mM HEPES, 20 mM $MgCl_2$, and 5 mM DTT. This mixture was incubated for 5 h; at 1 h intervals, the solution was mixed and a 100 $\mu$L aliquot was removed. These aliquots were clarified via centrifugation (5 min at 13 000 rpm in a benchtop microfuge), and the concentrations of the supernatant solutions were determined spectrophotometrically (see below). These determinations were repeated in triplicate. The concentration limits of hypoxanthine and xanthine were evaluated over the maximum time used for the assays (Table 1).

Concentrations were determined spectrophotometrically using a Cary Bio-100 spectrophotometer. Values of the absorption coefficient for each compound varied widely in the literature and were pH-dependent. For accurate concentration determination, an absorption coefficient was experimentally determined in the buffer solution used for the TGT assays. A stock solution of 500 mg of each compound was dissolved in dilute NaOH, and the pH of the solution was adjusted to 7.3. Serial dilutions were made, and a standard curve was generated from a plot of absorption versus concentration. The absorption coefficient was calculated from the slope of the line (e.g., slope divided by path length). Obtained values of absorption coefficients were similar to those previously reported.

Table 2: Experimental Conditions for Kinetic Determinations for Hypoxanthine and Xanthine[a]

| enzyme | [hypoxanthine] ($\mu$M) | [xanthine] ($\mu$M) | time course (both substrates) |
|---|---|---|---|
| htTGT(wt) | 25−3000 | 10−1500 | 120 min |
| htTGT(D143A) | 50−2000 | 1−750 | 120 min |
| htTGT(D143N) | 50−2000 | 0.5−750 | 120 min |
| htTGT(D143S) | 1−3000 | 1−3000 | 4 h |
| htTGT(D143T) | 1−3000 | 1−3000 | 4 h |

[a] [tRNA] = 20 $\mu$M for all enzymes, and [TGT] = 100 nM for all except htTGT(D143S) and htTGT(D143T) (250 nM). Assays were conducted in 100 mM HEPES (pH 7.3), 20 mM $MgCl_2$, and 5 mM DTT at 37 °C as described in Materials and Methods.

*Determination of Kinetic Parameters for Hypoxanthine and Xanthine.* The TGT-catalyzed incorporation of xanthine and hypoxanthine into tRNA was monitored by following the incorporation of radioactivity from tritium-labeled xanthine and hypoxanthine into tRNA as previously described for labeled guanine (*9*). $K_M$, $k_{cat}$, and $k_{cat}/K_M$ for hypoxanthine and xanthine were determined for htTGT(wt), htTGT(D143A), htTGT(D143N), htTGT(D143S), and htTGT(D143T). Therefore, tRNA was kept at a saturating (20 $\mu$M) concentration (see Results) for the $K_M$ and $k_{cat}$ determinations for hypoxanthine and xanthine.

htTGT(wt) (100 nM) was incubated with tRNA (20 $\mu$M) in the presence of radiolabeled [$^3$H]hypoxanthine or [$^3$H]xanthine (varied concentrations), $MgCl_2$ (20 mM), DTT (5 mM), and HEPES (100 mM) at pH 7.3 in a total reaction volume of 400 $\mu$L. At varying intervals over an appropriate time course (10−180 min, longer time course for less active enzymes), 70 $\mu$L aliquots were withdrawn and quenched in 2 mL of 5% TCA. This reaction mixture was allowed to precipitate for 1 h. The precipitated tRNA was then collected on Whatman GF/C glass microfiber filters. The filters were dried, and the radioactivity was counted via liquid scintillation to quantitate incorporation of [$^3$H]hypoxanthine or [$^3$H]xanthine into tRNA. The assays were performed, at least, in triplicate.

To determine the kinetic parameters for xanthine and hypoxanthine for wild-type and D143 mutant TGTs, various concentrations of xanthine and hypoxanthine and differing time courses, depending upon the enzyme, were used (Table 2). Note that the high concentrations of hypoxanthine were found to adsorb to the glass filters and cause inaccurately high and unstable readings of radioactivity. To prevent this, all filters used for hypoxanthine kinetics were presoaked in unlabeled hypoxanthine (2.5 mM) dissolved in 5% TCA and dried. All substrates were tested to their maximal level of solubility. Reaction time courses were followed to a maximum of 10% turnover, and the enzyme concentration was never greater than 0.1 times the substrate concentration. Initial velocities were determined via linear fits of radioactivity (converted to picomoles of xanthine or hypoxanthine using the appropriate specific activity) versus time. The initial velocities were then plotted against the concentration of the varied substrate. $K_M$ and $k_{cat}$ were calculated (averages of

three independent determinations) from nonlinear fits of the initial velocity data to the Michaelis−Menten equation. All relative values were determined relative to htTGT(wt). The efficiency constants, defined as $k_{cat}/K_M$, were also calculated. All errors are the standard errors of the fits with the errors in $k_{cat}/K_M$ normally propagated from the standard errors in $K_M$ and $k_{cat}$.

*Determination of $K_i$ Values for Xanthine.* htTGT(D143S) or htTGT(D143T) (200 nM) was incubated with tRNA (20 $\mu$M) in the presence of $MgCl_2$ (20 mM), DTT (5 mM), HEPES (100 mM, pH 7.3), [$^3$H]guanine (20−100 $\mu$M), and xanthine (25−500 $\mu$M) in a total reaction volume of 400 $\mu$L. Aliquots (70 $\mu$L) were taken at 15 min intervals over a 75 min time course. The aliquots were withdrawn, filtered, and quantified as described above. Initial velocities were calculated from linear fits of plots of the amount of guanine incorporated versus time. The initial velocities were replotted, and fit by three-dimensional, nonlinear regression to a competitive (with respect to guanine) inhibition equation (eq 1) using the preprogrammed equations in GraFit (*10*). The results were then plotted using Kaleidagraph to graphically display both the data and the fitted lines.

$$v_i = \frac{V_{max}[S]}{K_M(1 + [I]/K_i) + [S]} \quad (1)$$

$$\frac{1}{v_i} = \frac{K_M}{V_{max}[S]K_i}[I] + \frac{1}{V_{max}}\left|1 + \frac{K_M}{[S]}\right| \quad (2)$$

$$\frac{[S]}{v_i} = \frac{K_M}{V_{max}K_i}[I] + \frac{1}{V_{max}}([S] + K_M) \quad (3)$$

For graphical analysis of the data, eq 1 can be rearranged in the form of $1/v_i$ versus [I] (a Dixon plot, eq 2) (*11*) or $[S]/v_i$ versus [I] (the Cornish−Bowden method, eq 3) (*12*). In fact, both plots are complementary when analyzing data such as these. Therefore, the data were plotted by both methods on the basis of the methodology described below. In the case of competitive inhibition, plots of $1/v_i$ versus [I] (eq 2) are intersecting. Plots of $[S]/v_i$ versus [I] (eq 3) are parallel (the [S] term in the slope falls out of the equation, and the slope is a constant independent of [S]).

## RESULTS

*Kinetic Characterization of Wild-Type and Mutant TGTs with Hypoxanthine and Xanthine.* The kinetic parameters ($K_M$ and $k_{cat}$) for htTGT(wt), htTGT(D143A), and htTGT(D143N) were determined for hypoxanthine (Figures 2−4 and Table 3) and for xanthine (Figures 2−4 and Table 4). The incorporation of the alternate substrate was followed by monitoring the increase in $^3$H radioactivity in the tRNA caused by the exchange of an unlabeled guanine in position 34 of tRNA with a radiolabeled hypoxanthine or xanthine. It is reasonable to assume that the $K_M$ values of tRNA would not be affected by the nature of the heterocyclic substrate based on the ping-pong kinetic mechanism for TGT (*13*). The tRNA binds to TGT, and guanine 34 is then removed, forming a covalent tRNA−TGT intermediate. The incoming base then binds to the tRNA−TGT complex and is inserted into the tRNA in position 34, and the tRNA dissociates from the TGT. We have previously shown that the $K_M$ values for

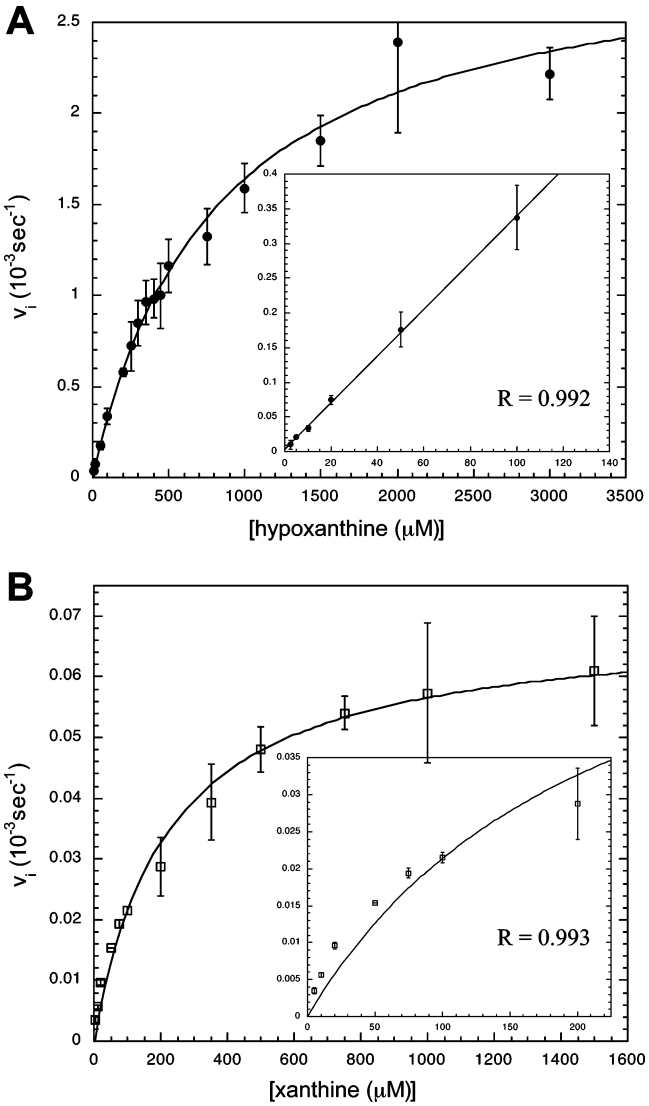


FIGURE 2: Michaelis−Menten kinetic plots for htTGT(wt): (A) kinetic fit for hypoxanthine and (B) kinetic fit for xanthine. Curves were obtained from a nonlinear fit of the average of three independent determinations of initial velocity data. Error bars are generated from the standard deviation in each point. The inset is an expansion of the low concentration. The fit of the curve is represented by *R*. Note that the scales of the axes change from plot to plot.

tRNA for each of these mutants are not significantly different from those for the wild-type TGT when studied with guanine (*4*). To confirm this, we have determined that at 10 $\mu$M, 20 $\mu$M (saturating, $10K_M$), and 40 $\mu$M tRNA, the rate of the reaction for both xanthine and hypoxanthine with each mutant TGT did not change (data not shown). For both the serine and threonine mutants, neither xanthine nor hypoxanthine exhibited any detectable substrate activity at concentrations up to the limit of their solubility.

The insets on each plot of the kinetics with hypoxanthine (Figures 2−4) show an independent linear fit of the low-concentration range to determine $k_{cat}/K_M$. This additional validation of the kinetic parameters determined from the Michaelis−Menten equation was necessary because saturating concentrations ($10K_M$) could not be reached due to the limit of solubility (ca. 2 mM, as discussed above). The determination of $k_{cat}/K_M$ using the linear fit of the data matched the $k_{cat}/K_M$ calculated from the kinetic parameters

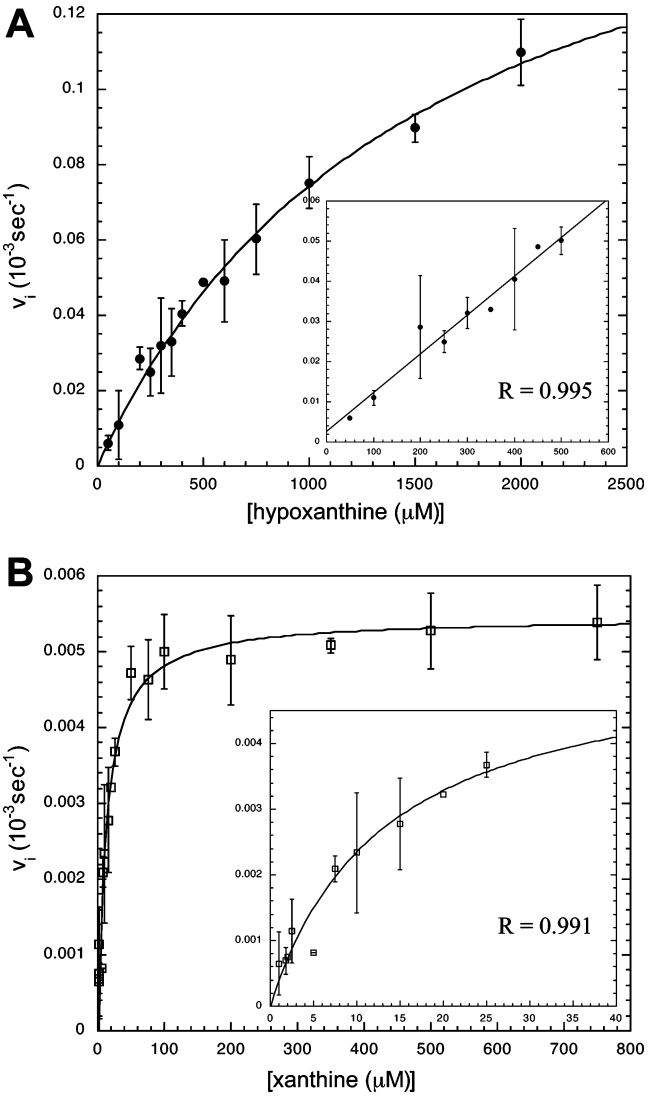


FIGURE 3: Michaelis−Menten kinetic plots for htTGT(D143A): (A) kinetic fit for hypoxanthine and (B) kinetic fit for xanthine. See the Figure 2 legend.

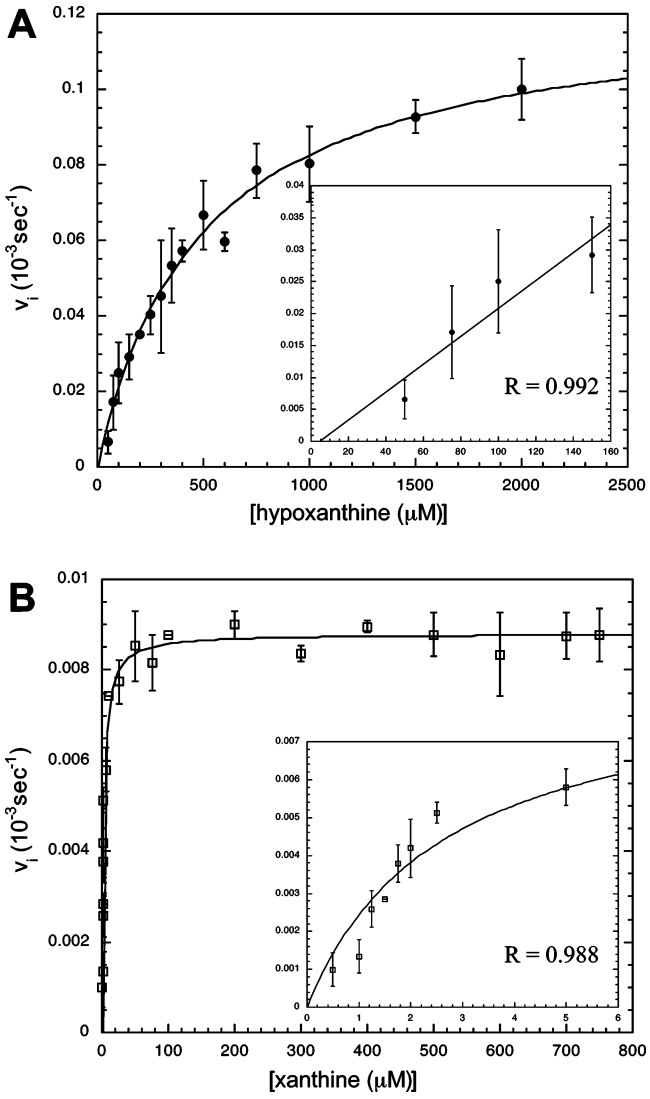


FIGURE 4: Michaelis−Menten kinetic plots for htTGT(D143N): (A) kinetic fit for hypoxanthine and (B) kinetic fit for xanthine. See the Figure 2 legend.

derived from the fits to the Michaelis−Menten equation (data not shown). On each plot of xanthine kinetics is an inset of the low-concentration range to better depict how well the data fit to the Michaelis−Menten equation.

*Inhibition of the D143S and D143T Mutants by Xanthine.* The inhibition constants for xanthine with htTGT(D143S) and htTGT(D143T) have been determined (Figures 5 and 6 and Table 4) by monitoring their ability to inhibit the incorporation of radiolabeled guanine into tRNA. For both htTGT(D143S) and htTGT(D143T), xanthine was found to be competitive, with respect to guanine, based on intersecting lines in a Dixon plot (Figures 5A and 6A) and parallel lines when plotted according to the Cornish−Bowden method (Figures 5B and 6B). The competitive inhibition constant ($K_i$) for htTGT(D143S) was 120 $\mu$M and for htTGT(D143T) was 90 $\mu$M; the data were calculated from the point of intersection in the Dixon plot. There was no inhibition seen with hypoxanthine.

## DISCUSSION

Previously, X-ray structural (*3*), biochemical (*4*), and computational (*4*) studies have all indicated that aspartate 143 is critical to the recognition of the 2-aminopyrimidin-4-one portion of the heterocyclic substrates for tRNA-guanine transglycosylase (TGT). This recognition is absolutely requisite for maintaining the proper Watson−Crick base pairing in the queuine-containing tRNAs anticodons, and hence the fidelity of translation of the corresponding codons. Given the critical role of aspartate 143, it seemed likely that mutants of aspartate 143 may exhibit altered heterocyclic substrate recognition properties. Therefore, we have examined the recognition of xanthine and hypoxanthine by wild-type and D143 mutant TGTs.

We have previously reported the construction and biochemical and computational characterization of these mutants and their interactions with guanine (*4*). Consistent with the postulate that heterocyclic substrate specificity is critical for the proper functioning of the corresponding tRNAs, we observed that the D143 mutants could be expressed only in the presence of chromosomally encoded wild-type TGT (which presumably maintained the integrity of the tRNAs). The mutants were expressed in histidine-tagged form to allow for purification away from the contaminating wild type. The mutants exhibited an increasing trend in $K_M$ for guanine.

Table 3: Hypoxanthine Kinetic Parameters for TGTs

| enzyme | $k_{cat}^{a,b,d}$ ($\times 10^{-6}$ s$^{-1}$) | $K_M^{a,b,d}$ ($\mu$M) | $k_{cat}/K_M^{a,b,d}$ ($\times 10^{-6}$ s$^{-1}$ $\mu$M$^{-1}$) | relative $K_M^{a,c,d}$ | relative $k_{cat}/K_M^{a,c,d}$ |
|---|---|---|---|---|---|
| htTGT(wt) | 2970 (140) | 811 (86) | 3.7 (0.4) | 1.0 | 1.0 |
| htTGT(D143A) | 190 (13) | 1550 (170) | 0.1 (0.02) | 1.9 | 0.03 |
| htTGT(D143N) | 120 (05) | 490 (45) | 0.2 (0.02) | 0.6 | 0.07 |
| htTGT(D143S) | NA[e] | NA[e] | – | – | – |
| htTGT(D143T) | NA[e] | NA[e] | – | – | – |

[a] Standard errors are given in parentheses. [b] Kinetic parameters are calculated from the average of three replicate determinations of initial velocity data. [c] Relative values were determined relative to that of the His-tagged wild type. [d] The error was calculated as detailed in Materials and Methods and described in refs *20* and *21*. [e] No activity within the limits of solubility (2 mM hypoxanthine).

Table 4: Xanthine Kinetic Parameters for TGTs

| enzyme | $k_{cat}^{a,b,d}$ ($\times 10^{-6}$ s$^{-1}$) | $K_M^{a,b,d}$ ($\mu$M) | $k_{cat}/K_M^{a,b,d}$ ($\times 10^{-6}$ s$^{-1}$ $\mu$M$^{-1}$) | relative $K_M^{a,c,d}$ | relative $k_{cat}/K_M^{a,c,d}$ |
|---|---|---|---|---|---|
| htTGT(wt) | 69 (3) | 224 (28) | 0.31 (0.04) | 1.0 | 1.0 |
| htTGT(D143A) | 5.5 (0. 1) | 13 (1) | 0.42 (0.04) | 0.059 | 1.35 |
| htTGT(D143N) | 8.8 (0.1) | 2.6 (0.2) | 3.4 (0.3) | 0.012 | 10.9 |
| htTGT(D143S) | NA[e] | – | – | – | – |
| htTGT(D143T) | NA[e] | – | – | – | – |

[a] Standard errors are given in parentheses. [b] Kinetic parameters are calculated from the average of three replicate determinations of initial velocity data. [c] Relative values were determined relative to that of the His-tagged wild type. [d] The error was calculated as detailed in Materials and Methods and described in refs *20* and *21*. [e] No activity within the limits of solubility (1.5 mM xanthine).

Given that TGT follows the ping-pong kinetics with guanine binding second (*13*) and assuming that a step after guanine binding is rate-limiting [for which we have evidence (*14*)], then the $K_M$ for guanine is very likely to be equivalent to its $K_D$ and can be treated as a measure of binding affinity and/or recognition. These results clearly demonstrated that asparate 143 is intimately involved in recognizing guanine.

Hypoxanthine and xanthine were selected because they are close analogues of guanine, a well-characterized substrate for TGT, and because they are naturally occurring, physiologically relevant molecules. In vivo, TGT must be able to discriminate against hypoxanthine and xanthine in favor of its natural substrate queuine (or preQ$_1$). Perhaps more importantly, hypoxanthine and xanthine differ from guanine in the 2-aminopyrimidin-4-one portion of the molecule, the exact portion that is recognized by aspartate 143. Therefore, they are the logical choices to use to probe the differential substrate recognition properties of aspartate 143 mutants of TGT. Figure 7 shows the interactions between guanine and wild-type and D143 mutant TGTs as previously determined by biochemical and computational studies (*4*). On the basis of a manual hydrogen bonding analysis, we have selected those TGT mutants which seem likely to have the highest affinity for hypoxanthine and xanthine. The expected interactions between these mutants and hypoxanthine and xanthine are also displayed in Figure 7. Most interestingly, the D143N mutant is predicted to restore the hydrogen bond that is lost between wild-type TGT and xanthine relative to guanine.

In-depth biochemical analyses for xanthine and hypoxanthine were carried out to explore the recognition of these alternate bases by wild-type and D143 mutant TGTs. Some unexpected results were obtained. Hypoxanthine was not recognized, as initially hypothesized, by htTGT(D143S) or htTGT(D143T). Xanthine was found to act as a substrate with the wild type, htTGT(D143A), and htTGT(D143N), but unexpectedly as an inhibitor of htTGT(D143S) and htTGT(D143T). Initially, it was expected that the overall affinity of htTGT(D143N) for xanthine would be comparable to the affinity of the wild type for guanine. However, the overall catalytic efficiency ($k_{cat}/K_M$) of htTGT(D143N) with xanthine was much lower than that for the wild type with guanine. This was due to a substantial and unexpected decrease in $k_{cat}$.

*Recognition of Hypoxanthine.* The recognition of hypoxanthine, relative to that for guanine and xanthine, by wild-type and all D143 mutant TGTs was poor (Tables 3−5). It is interesting to note that the catalytic rates of the reactions, $k_{cat}$, observed for the wild type, D143A, and D143N with hypoxanthine were similar to those observed with guanine [2300, 380, and 580 $\times$ $10^{-6}$ s$^{-1}$, respectively (*4*)]. The serine (D143S) and threonine (D143T) TGT mutants were initially hypothesized to exhibit a strong binding preference for hypoxanthine, but within the limits of detection and at concentrations up to its solubility limit, hypoxanthine was not a substrate for TGT(D143S) or TGT(D143T). Given the similarity of the $k_{cat}$ values for hypoxanthine and guanine with the wild type and the alanine and asparagine mutants, it is clear that, once bound, hypoxanthine is a good substrate for the chemical steps in the TGT reaction. Therefore, it is likely that the inactivity of hypoxanthine with the serine and threonine mutants is due to very poor binding and/or recognition.

*Recognition of Xanthine as a Substrate.* Biochemical characterization of the interaction between TGT (wild-type and D143 mutants) and xanthine demonstrates that xanthine is better recognized than hypoxanthine by all TGTs (Tables 3−5). The alanine mutant (D143A), which was initially expected to recognize guanine and xanthine similarly, does indeed exhibit comparable values of $K_M$ (Table 5) for both substrates.

The asparagine mutant (D143N) was hypothesized to have an affinity for xanthine comparable to that of the wild type for guanine, suggesting a potential inversion of substrate specificity. Indeed, the experimental data clearly indicate that an inversion of specificity (in terms of $K_M$) was seen with the D143N mutant recognizing xanthine in preference over

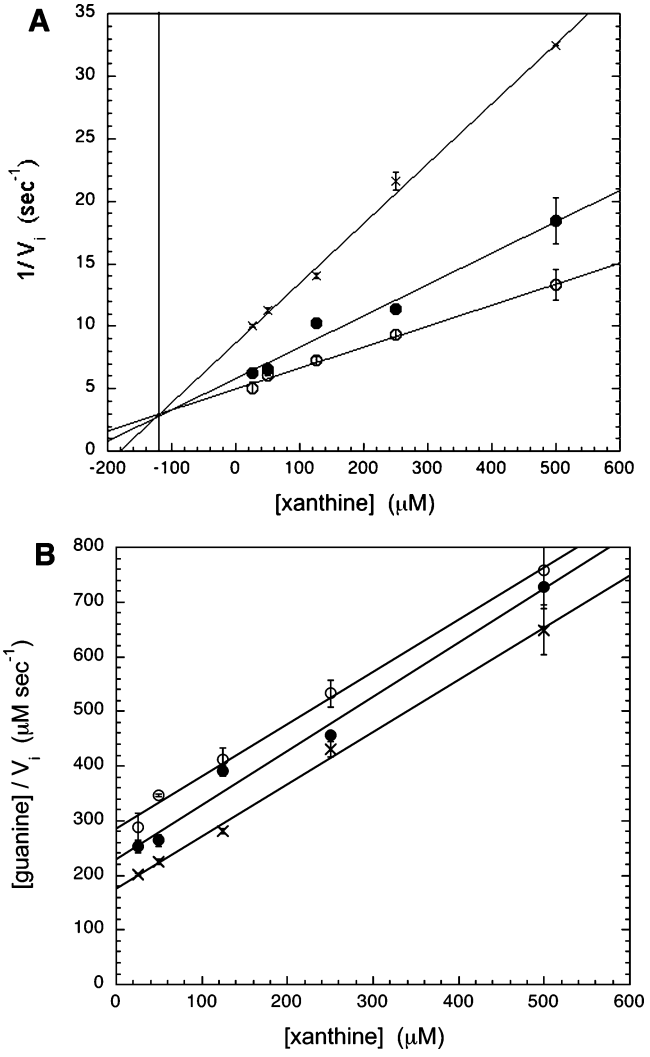


FIGURE 5: Plots of inhibition of htTGT(D143S) by xanthine: (A) Dixon plot and (B) Cornish−Bowden plot. The mode of inhibition of incorporation of guanine by xanthine was determined by varying the concentrations of xanthine (25−500 $\mu$M), while holding tRNA constant at a saturating concentration (20 $\mu$M) at three different concentrations of guanine [(○) 20, (●) 40, and (×) 57 $\mu$M]. The data were analyzed graphically by plotting either (A) $1/v_i$ vs [xanthine] (eq 2) or (B) [guanine]/$v_i$ vs [xanthine] (eq 3). $K_i$ (competitive with respect to guanine) corresponds to the point of intersection in the Dixon plot (A). The data points arise from an average of two independent determinations of initial velocities under these conditions.

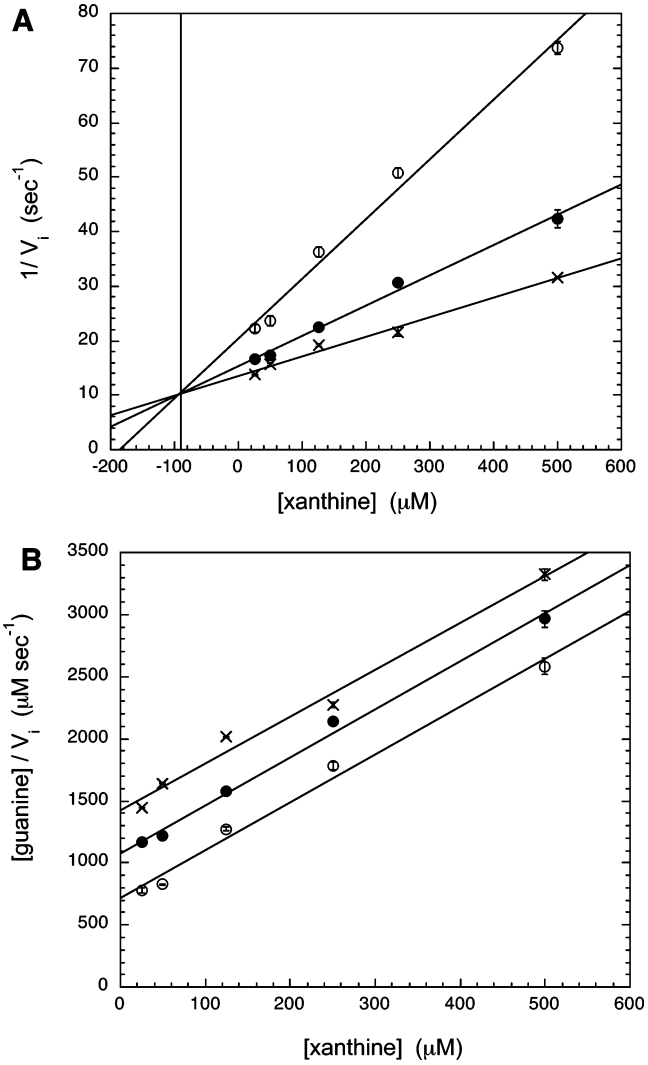


FIGURE 6: Plots of inhibition of htTGT(D143T) by xanthine: (A) Dixon plot and (B) Cornish−Bowden plot. The mode of inhibition of guanine kinetics by xanthine was determined by varying the concentrations of xanthine (25−500 $\mu$M), while holding tRNA constant at a saturating concentration (20 $\mu$M) at three different concentrations of guanine [(○) 35, (●) 70, and (×) 105 $\mu$M]. The data were analyzed as described in the legend of Figure 5.

guanine (Table 5). The expected hydrogen bonding pattern of xanthine bound to D143N closely mimics that of guanine bound to the wild type, suggesting that the positioning of and the interactions with the substrate are similar (Figure 7). An investigation by Kang et al. (*6*), involving *E. coli* adenylosuccinate synthetase (AMPSase), yielded a similar inversion of specificity. They established that the determinant of AMPSase for guanosine 5′-triphosphate specificity is D333, and mutating this residue to asparagine alters substrate specificity from GTP to XTP. They proposed that the aspargine mutant most likely makes complementary hydrogen bonds to XTP, accepting a hydrogen onto the 2-oxo group and donating a hydrogen from the N1 position of the base of XTP (*6*).

Although the hydrogen bonding patterns for the wild type with guanine and D143N with xanthine are almost identical, their $K_M$ values are significantly different. It is likely that this is, in part, due to differences in the strengths of the hydrogen bonds in which they take part. The wild-type D143 side chain has two oxygens that share a negative charge. This carboxylate provides two hydrogen bond acceptors with a formal negative charge. Guanine has two nitrogens (one amine and one amide) which donate hydrogen bonds. The mutant D143N side chain has a neutral amide group that provides one hydrogen bond donor (nitrogen) and one acceptor (oxygen). Xanthine also has an amide group within the structure of the ring that provides the complementary hydrogen bond acceptor (amide oxygen) and donor (amide nitrogen).

In contrast, Munagala and Wang discovered that a mutation from aspartate 163 to asparagine resulted in a loss of specificity for xanthine in HGXPRTase (hypoxanthine-guanine-xanthine phosphoribosyltransferase), whereas the recognition of guanine and hypoxanthine remained unaltered (*15*). On the basis of a crystal structure of xanthine bound to *Tritrichomonas foetus* HGXPRTase, aspartate 163 rec-

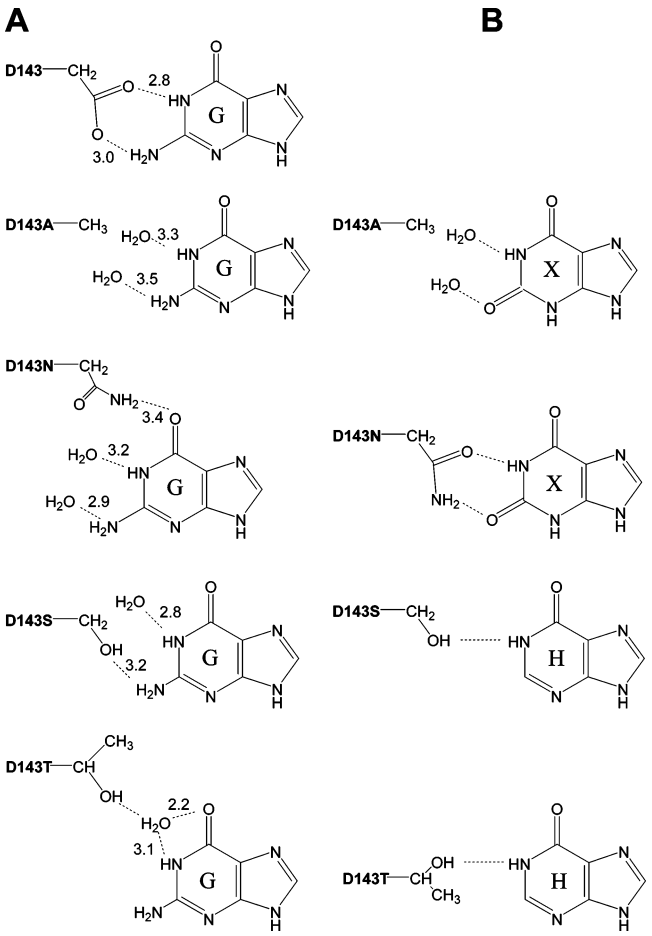


FIGURE 7: Recognition of guanine (A) by the D143 mutant TGTs and the alternate purine substrates (B) paired with their presumptively most appropriate mutant (G denotes guanine, X xanthine, and H hypoxanthine).

Table 5: Comparison of Experimental $K_M$ and $K_i$ Values of Guanine, Hypoxanthine, and Xanthine with TGTs

| enzyme | guanine $K_M$ ($\mu$M) | hypoxanthine $K_M$ ($\mu$M) | xanthine $K_M$ or $K_i$ ($\mu$M) |
|---|---|---|---|
| htTGT(wt) | 0.15[a] | 811 | 224 |
| htTGT(D143A) | 11.4 | 1550 | 13.2 |
| htTGT(D143N) | 21.8 | 490 | 2.6 |
| htTGT(D143S) | 57 | NA[b] | 109 (17)[c] |
| htTGT(D143T) | 105 | NA[b] | 75 (11)[c] |

[a] Data from ref *4*. [b] No activity was determined given the limits of substrate solubility (2 mM for hypoxanthine and 1.5 mM for xanthine). [c] For the serine and threonine mutants, xanthine was found to competitively inhibit the incorporation of guanine. Values were determined via a nonlinear regression fit to a competitive inhibition model (eq 2). Note that the errors in the $K_M$ values (which are found in Tables 3 and 4) have been omitted here for clarity.

ognizes O2 of xanthine via a water-mediated hydrogen bond (*15*). The amide of asparagine would not be expected to participate in such a water-mediated hydrogen bond, accounting for the loss of xanthine recognition in this case.

*Recognition of Xanthine as an Inhibitor.* Interestingly, xanthine was found to act as an inhibitor, competitive with respect to guanine, for TGT(D143S) and TGT(D143T) (Figures 5 and 6 and Table 4). It is very interesting that xanthine inhibits D143S and D143T more efficiently than xanthine acts as a substrate for wild-type TGT (Table 5). Xanthine exhibits a kind of pseudosymmetry around its 2,4-

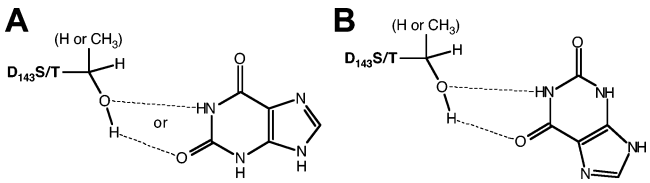


FIGURE 8: Potential pseudosymmetric binding modes between TGT(D143S/T) and xanthine: (A) "normal" binding mode and (B) "nonproductive" binding mode.

dioxopyrimidine moiety. It is possible that xanthine may bind in an alternative, nonproductive mode to these two TGT mutants (Figure 8). If this is true, it may also explain the reduced $k_{cat}$ values for xanthine with wild-type and other D143 mutant TGTs (see below).

*Reduction in $k_{cat}$ for Xanthine.* The biochemical studies with xanthine reveal that, although the $k_{cat}$ values for hypoxanthine are similar to those for guanine, the values for xanthine decrease 30-fold (wild-type) to 70-fold (D143 mutants) relative to those for guanine. The first half of the TGT reaction is identical for all heterocyclic substrates: the tRNA binds, and G34 of tRNA is displaced and dissociates, resulting in a covalent TGT−tRNA complex (*16*). The second half of the reaction involves heterocyclic substrate binding, deprotonation of the N9 position of the base, and, last, attack of the ribose displacing TGT by the base. The rate-limiting step of this reaction is unknown, but evidence suggests that it occurs after the formation of the covalent intermediate (*14*). It is possible that the rate-limiting step for the reaction may change with a change the heterocyclic substrate. Therefore, it is difficult to definitively explain the decrease in $k_{cat}$ for xanthine with wild-type and D143 mutant TGTs. However, there are four possibilities which may be considered: (1) the altered chemistry of the purine ring, (2) a potential slow release of xanthine-modified tRNA, (3) the binding of xanthine to cause a change in the active site affecting the position of catalytic residues, and (4) the potential for xanthine to act as both a substrate and an inhibitor.

The first possibility is that since the chemistry of the ring is altered by substitution of a carbonyl oxygen (xanthine) for an amine (guanine) on C2, this may affect the reactivity of xanthine in the chemical steps of the TGT reaction. If the p$K_a$ of the N9 position is higher, it may be more difficult to deprotonate the incoming base, thereby slowing the reaction. However, the first p$K_a$ (i.e., neutral species to anionic) of xanthine is within 1 p$K_a$ unit of that of guanine (9.9 and 9.26, respectively) (*17*), inconsistent with a 30−70-fold decrease in $k_{cat}$. For HGXPRTase, Munagala and Wang (*15*) found that the $k_{cat}$ values of the conversion from the bases (hypoxanthine, guanine, and xanthine) to the nucleotide monophosphates (IMP, GMP, and XMP) are very similar (8.9, 2.5, and 4.8 $s^{-1}$, respectively). This reaction involves deprotonation of the base and formation of a glycosidic bond. These two steps are mimicked in the second half of the TGT reaction (*16*) in which the incoming base (guanine, hypoxanthine, or xanthine) is deprotonated. This base then attacks the TGT−tRNA complex, displacing TGT and forming a glycosidic bond. In the case of HGXPRTase, the $k_{cat}$ value of hypoxanthine is ca. 3-fold decreased relative to that for guanine. This result is mirrored by the minor differences we have observed in the $k_{cat}$ values of hypoxanthine relative to

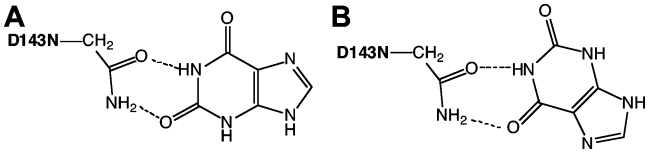


FIGURE 9: Potential binding modes between TGT(D143N) and xanthine: (A) normal binding mode and (B) nonproductive binding mode.

guanine for TGTs (wild type and D143 mutants) (Tables 3 and 4). In HGXPRTase, the $k_{cat}$ value of xanthine is decreased ca. 2-fold relative to that of guanine, suggesting that it is unlikely that differences in the heterocyclic ring chemistry are responsible for the significant reductions in $k_{cat}$ that we have observed for xanthine relative to guanine.

The second possibility is that if product release is the rate-limiting step for the xanthine reaction, then a slow dissociation of the xanthine(34)-tRNA·TGT complex would result in a lower $k_{cat}$. This is unlikely since the tRNA has multiple interactions, and one small binding interaction would most likely result in little contribution to the binding. Additionally, Goodenough-Lashua investigated the binding of guanine(34)-tRNA and $preQ_1$(34)-tRNA (*18*). It was determined that $preQ_1$(34)-tRNA binds 2-fold more tightly than guanine(34)-tRNA; however, the rates of the reactions of TGT with guanine versus those with $preQ_1$ were previously determined to be comparable (*19*).

The third possibility is that a reorganization of the active site residues occurs upon xanthine binding. It was previously discussed (*4*) that D143 is involved in a key hydrogen bond with S90; this hydrogen bond orients S90, which, in turn, orients both the substrate and a catalytic residue, D89. In computational simulations of the D143 mutants with guanine, S90 moves 2−3 Å away from guanine in comparison to its position in the wild type (*4*). This was proposed to be the reason that the mutants exhibited a 10-fold decrease in activity relative to wild-type TGT. It is certainly possible that the binding of xanthine causes a reorganization of active site residues S90 and D89, thereby causing a decrease in $k_{cat}$ values for the incorporation of xanthine.

The fourth and perhaps most likely possibility is that xanthine may act as both a substrate and an inhibitor. Inhibition may occur via xanthine binding in a 180°-flipped conformation because of the pseudosymmetry of the molecule (Figure 9). This binding orientation would position N9 such that it could not be deprotonated in the normal reaction and would therefore result in a nonproductive binding mode. Above, we postulated that this type of binding mode may be responsible for the xanthine inhibition of TGT(D143S) and TGT(D143T) that we have observed. For these mutants, the changes in the active site may have enhanced the affinity of xanthine for this nonproductive binding mode to the extent that no normal reaction is seen. For the wild type and other D143 mutants, both binding modes may have similar affinities, resulting in a lower $k_{cat}$ due to the presumed nonproductive binding. Further studies are necessary to clarify this issue.

As one final note, we have previously developed and used a computational model system to probe the molecular details of the interaction between guanine and wild-type and D143 mutant TGTs (*4*). However, attempts to computationally model the interaction of xanthine with wild-type and D143 mutant TGTs (K. A. Todorov, X.-J. Tan, G. A. Garcia, and H. A. Carlson, unpublished observations) were unsuccessful in correlating the predicted free energies of binding with the observed values. It should be noted that the modeling was carried out for a time frame (1 ns) that is not sufficient to allow the xanthine to flip into the alternate, nonproductive binding mode that we postulate. Given that, it is not surprising that the calculations do not correlate with experiment in the xanthine case. In fact, this is consistent with our nonproductive binding mode hypothesis.

Our results have provided further confirmation of the important role that aspartate 143 plays in heterocyclic substrate recognition in the TGT reaction. The inversion of recognition of xanthine over guanine that we have observed for the asparagine mutant indicates that it is possible that TGT could be engineered to incorporate a base with different Watson−Crick-type base pairing properties into tRNA. If this were done in conjunction with altered tRNA recognition, then a novel tRNA with a novel anticodon wobble base could theoretically be generated in vivo and could be used to study genetic code evolution and perhaps in unnatural amino acid mutagenesis.

## ACKNOWLEDGMENT

We thank Dr. Jeff Kittendorf for critical review of the experimental procedures and results reported in this paper.

## REFERENCES

1. Grosjean, H., and Benne, R. (1998) *Modification and Editing of RNA: The Alteration of RNA Structure and Function*, ASM Press, Washington, DC.
2. Iwata-Reuyl, D. (2003) Biosynthesis of the 7-deazaguanosine hypermodified nucleosides of transfer RNA, *Bioorg. Chem. 31*, 24−43.
3. Romier, C., Reuter, K., Suck, D., and Ficner, R. (1996) Crystal structure of tRNA-guanine transglycosylase: RNA modification by base exchange, *EMBO J. 15*, 2850−2857.
4. Todorov, K., Tan, X.-J., Nonekowski, S. T., Garcia, G. A., and Carlson, H. A. (2005) The Role of Aspartic Acid 143 in *E. coli* tRNA-Guanine Transglycosylase: Insights from Mutagenesis Studies and Computational Modeling, *Biophys. J. 89*, 1965−1977.
5. Reyes, C. M., and Kollman, P. A. (2000) Investigating the Binding Specificity of U1A-RNA by Computational Mutagenesis, *J. Mol. Biol. 295*, 1−6.
6. Kang, C., Sun, N., Honzatko, R. B., and Fromm, H. J. (1994) Replacement of $Asp^{333}$ with Asn by Site-directed Mutatgenesis Changes the Substrate Specificity of *Escherichia coli* Adenylosuccinate Synthetase from Guanosine 5′-Triphosphate to Xanthosine 5′-Triphosphate, *J. Biol. Chem. 269*, 24046−24049.
7. Zhong, J.-M., Chen-Hwang, M.-C., and Hwang, Y.-W. (1995) Switching Nucleotide Specificity of Ha-Ras p21 by a Single Amino Acid Substitution at Aspartate 119, *J. Biol. Chem. 270*, 10002−10007.
8. Curnow, A. W., Kung, F. L., Koch, K. A., and Garcia, G. A. (1993) tRNA-Guanine Transglycosylase from *Escherichia coli*: Gross tRNA Structural Requirements for Recognition, *Biochemistry 32*, 5239−5246.
9. Okada, N., and Nishimura, S. (1979) Isolation and Characterization of a Guanine Insertion Enzyme, a Specific tRNA Transglycosylase, from *Escherichia coli*, *J. Biol. Chem. 254*, 3061−3066.
10. Leatherbarrow, R. (1990) *GraFit Users Manual*, 2nd ed., Erithacus Software Ltd., Staines, U.K.
11. Dixon, M. (1953) The Determination of Enzyme Inhibitor Constants, *Biochem. J. 56*, 170−171.
12. Cornish-Bowden, A. (1974) A Simple Graphical Method for Determining the Inhibition Constants of Mixed, Uncompetitive, and Non-Competitive Inhibitors, *Biochem. J. 137*, 143−144.
13. Goodenough-Lashua, D. M., and Garcia, G. A. (2003) tRNA-Guanine Transglycosylase from *Escherichia coli*: A Ping-Pong

Kinetic Mechanism is Consistent with Nucleophilic Catalysis, *Bioorg. Chem. 31*, 331−344.
14. Kittendorf, J. D. (2004) PhD dissertation in *Medicinal Chemistry*, University of Michigan, Ann Arbor, MI.
15. Munagala, N. R., and Wang, C. C. (1998) Altering Purine Specificity of Hypoxanthin-Guanine-Xanthine Phosphoribosyltransferase from *Trichomonas foetus* by Structure-Based Point Mutations in the Enzyme Protein, *Biochemistry 37*, 16612−16619.
16. Garcia, G. A., and Kittendorf, J. D. (2005) Transglycosylation: A mechanism for RNA modification (and editing?), *Bioorg. Chem. 33*, 229−251.
17. Windholz, M., Budavari, S., Blumetti, R. F., and Otterbein, E. S. (1983) *The Merck Index*, 10th ed., Merck & Co., Inc., Rahway, NJ.
18. Goodenough-Lashua, D. M. (2002) PhD dissertation in *Medicinal Chemistry*, University of Michigan, Ann Arbor, MI.
19. Hoops, G. C., Townsend, L. B., and Garcia, G. A. (1995) tRNA-guanine transglycosylase from *Escherichia coli*: Structure−activity studies investigating the role of the aminomethyl substituent of the heterocyclic substrate preQ1, *Biochemistry 34*, 15381−15387.
20. Harris, D. C. (1991) *Quantitative Chemical Analysis*, 3rd ed., W. H. Freeman and Co., New York.
21. Gordon, A. J., and Ford, R. A. (1972) *The Chemist's Companion: A Handbook of Practical Data, Techniques, and References*, Wiley-Interscience, New York.

BI051863D